







How to cite: Angew. Chem. Int. Ed. 2021, 60, 8710-8716 International Edition: doi.org/10.1002/anie.202016384 German Edition: doi.org/10.1002/ange.202016384

Stable Thermotropic 3D and 2D Double Gyroid Nanostructures with Sub-2-nm Feature Size from Scalable Sugar-Polyolefin Conjugates

Samantha R. Nowak, Kätchen K. Lachmayr, Kevin G. Yager, and Lawrence R. Sita*

Abstract: Ultra-low molecular weight disaccharide-polyolefin conjugates with cellobiose, lactose and maltose head groups and atactic polypropene tails, such as 1, undergo a series of irreversible thermotropic order-order transitions with increasing temperature to provide nanostructured phases in the sequence: lamellar (L), hexagonal perforated lamellar (HPL), double gyroid (DG) and hexagonal cylindrical (C). The DG phase displays exceptional stability at ambient temperature and features two interpenetrating sugar domain networks having a sub-2-nm strut width and a lattice parameter, a_{DG} , of 13.1 nm. The unique stability of this DG phase extends further within ultrathin films all the way down to the two-dimensional limit of 15 nm in which film thickness, l, is now less than the surface-oriented unit cell height, h_{DG} . In addition to raising the fundamental question of what minimally constitutes a Schoen triply periodic minimal surface and DG lattice, these results serve to establish the class of sugarpolyolefin conjugates as a new material platform for nanoscience and nanotechnology.

he next revolutions in science and technology require the ability to fabricate, with high fidelity, nanostructured materials with sub-2-nm, feature size. [1] Single-digit nanofabrication of large-area periodic arrays should also ideally be amenable to high speed roll-to-roll manufacturing involving the selfassembly of robust nanostructures within sub-100 nm film thicknesses under non-stringent conditions, and ideally, using materials that can be obtained in practical quantities from inexpensive and sustainable precursors.[2] With respect to these goals, one of the most intriguing nanostructures is the cubic "double gyroid" (DG) phase that is based on the Schoen triply periodic minimal surface (TPMS) with $Ia\bar{3}d$ symmetry, shown in Figure 1, in which two enantiomorphic interpenetrating networks of a minority domain are separated and enclosed within a matrix provided by a majority phase. [3,4] Soft matter DG phases have previously been experimentally observed as a thermodynamically stable equilibrium state within the phase diagrams of molecular surfactants, liquid

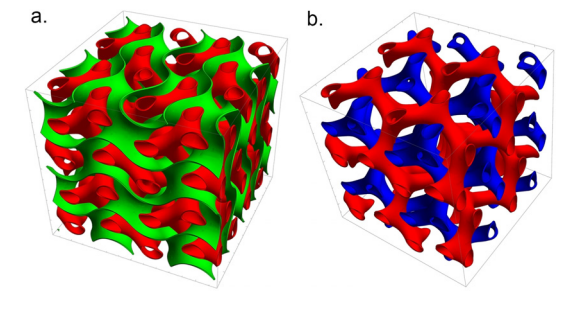
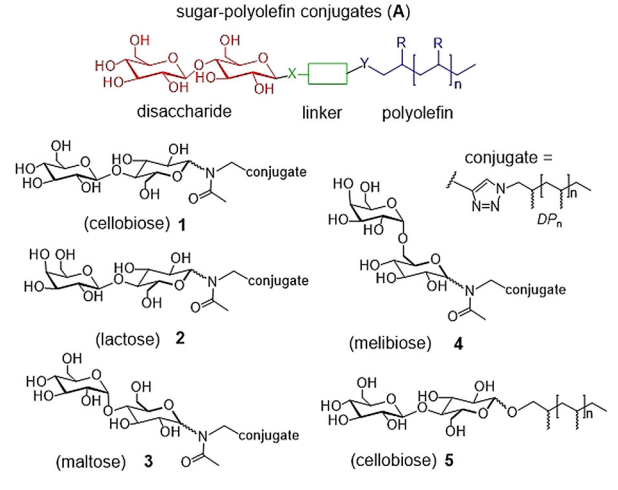


Figure 1. a) Mathematical approximate for the Schoen cubic double gyroid (DG) of $la\bar{3}d$ symmetry in which the triply periodic minimal surface (TPMS) (green) separates two interpenetrating channels (red). b) Same structure as in (a) but with TPMS removed to highlight the two enantiomorphic networks (red and blue).

crystals, glycolipids, block copolymers, and "giant" surfactants. [5] Templated nanofabrication using soft matter DGphases has also been used to generate "hard" gyroidal nanostructures with potential applications in the areas of photonics, metamaterials, supercapacitors, high density batteries, and solar energy cells, to name a few. [6] On the other hand, a condensed state soft matter DG phase with a sub-10nm feature size has yet to be observed that displays long-term stability under ambient conditions within ultrathin films that are less than 100 nm thick.^[7] Herein, we now report that readily-available and scalable sugar-polyolefin conjugates with the generic structure of A shown in Scheme 1 can be used to selectively access a range of thermotropic nanostructured phases in pure form in both the bulk and within ultrathin films through a series of well-defined, thermally-



Scheme 1. Structures of sugar-polyolefin conjugates 1-5.

Department of Chemistry and Biochemistry, University of Maryland College Park, MD 20742 (USA)

E-mail: lsita@umd.edu

Dr. K. G. Yager Center for Functional Nanomaterials Brookhaven National Laboratory Upton, NY 11973 (USA)

Supporting information and the ORCID identification number(s) for the author(s) of this article can be found under https://doi.org/10. 1002/anie.202016384.

^[*] S. R. Nowak, K. K. Lachmayr, Prof. Dr. L. R. Sita





induced order-order transitions. Importantly, it is established for several disaccharide-linked atactic polypropene (aPP) derivatives of A that highly ordered DG nanostructured ultrathin films with a sub-2-nm feature size are uniquely stable under ambient conditions in the absence of any interface modifications involving secondary "bottom" or "top coats". [7d,8,9] Additional results further show that both the structure of the disaccharide head group and the numberaverage degree of polymerization (DP_n) of the aPP tail in A play critical roles in dictating thermotropic phase behaviour and phase stability, while the structure of the linker and surface energy of the substrate for the ultrathin films do not appear to be significant governing factors. Finally, and most surprisingly, the stability of DG nanostructures of these disaccharide-aPP derivatives of A extends down to the twodimensional limit where film thickness, l, is now less than the value required to accommodate a complete unit cell lattice that is preferentially oriented with the (211) Miller planes aligned parallel to the substrate surface. In addition to raising the fundamental question of what minimally constitutes a Schoen TPMS DG lattice, these results serve to establish the class of sugar-polyolefin conjugates as a new material platform for nanoscience and nanotechnology.[10]

Using previously published methods, the sugar-polyolefin conjugates 1-4 of Scheme 1 were easily prepared through copper-mediated "click chemistry" between a corresponding disaccharide-based N-acetyl propargyl amide starting material and an ultra-low molecular weight, azido-terminated amorphous *atactic* polypropene (N₃-aPP) building block.^[10-12] The ether-linked cellobiose-aPP conjugate 5 was further obtained by employing standard carbohydrate synthetic methods and an ultra-low molecular weight hydroxy-terminated aPP (HO-aPP) precursor. [12] Importantly, both the N₃aPP and HO-aPP starting materials were, in turn, easily prepared with a tunable \overline{DP}_n value and very narrow molecular weight distribution, as evidenced by a polydispersity index, D $(=M_{\rm w}/M_{\rm p})$, that is typically < 1.1, through the living coordinative chain transfer polymerization (LCCTP) of propene followed by reactive quenching and end-group functionalization. [10,11] Finally, for each new sample of 1-5 that was separately synthesized, a combination of gel permeation chromatography (GPC), high-field 1D- and 2D ¹H and ¹³C NMR spectroscopy, and matrix-assisted laser desorption ionization (MALDI) mass spectrometry was used to establish the number-average and weight-average molecular weight indices, $M_{\rm n}$ and $M_{\rm w}$, $DP_{\rm n}$, and $\mathcal D$ values. [12] Here it must be pointed out that, due to the ultra-low molar masses of the aPP domains that are being targeted, slight synthetic variation in the molecular weight-related parameters of each sugarpolyolefin is unavoidable in going from one batch to another. On the other hand, since only large variations significantly impact phase behavior (vide infra), it was possible to use this synthetic and characterization methodology to create a series of derivatives for several of the disaccharide-aPP conjugates of Scheme 1 in order to investigate molecular-weight dependent trends in phase behavior by targeting 500 Da, 1000 Da and 2500 Da as the molar mass of the aPP domain. Finally, investigations of the bulk thermal properties of 1-5 using conventional differential scanning calorimetry (DSC) and thermogravimetric analysis (TGA) only revealed phase transitions that are dominated by the glass transition temperature, $T_{\rm g}$, of the aPP domain, and possibly that of the disaccharide in the former, while the latter confirmed that all of these sugar-polyolefin conjugates experience very little weight loss up to a temperature of 250°C whereupon the onset of significant decomposition occurs. [12]

In a preliminary report, we documented that, in the absence of any thermal history, a bulk sample of 1 with DP_n = 31 adopts a lamellar (L) phase as determined by small angle x-ray scattering (SAXS) acquired at room temperature. [10b] Phase-sensitive tapping mode atomic force microscopy (ps-AFM) and grazing incidence SAXS (GISAXS) investigations of freshly prepared ultrathin films of **1** for l < 100 nm that were deposited onto highly-oriented pyrolytic graphite (HOPG) or carbon-coated polycrystalline silicon (c-Si) substrates similarly revealed a lamellar mesophase with the domains initially oriented perpendicular to the surface (L_{\perp}) and with a domain spacing of 6.5 nm.[13] Quite surprisingly, however, a dynamic thermotropic structural reorganization of this L_{\perp} phase of 1 was observed to occur even at the relatively low temperature of 38°C to provide a new equilibrium morphology in which the lamellae are now oriented parallel to the surface (L_{\parallel}) . Following this facile $L_{\perp} \to L_{\parallel}$ structural reorganization through ps-AFM analysis of heated ultrathin films of 1 that were rapidly cooled at timed intervals provided tantalizing glimpses of nanostructured intermediate states. However, due to the capabilities of the analytical tools and limited temperature range that were employed at the time, no concrete structural interpretations of these intermediate phases could be established.

Intrigued by the facile dynamic structural reorganization displayed by 1, an extensive variable temperature synchrotron SAXS investigation was conducted on a newly synthesized sample, 1a, with $DP_n = 17$ (D = 1.03) by employing different temperature ramp and jump profiles during which new data was collected using a 10 second exposure time at each sample location as it was rastered between data collections in order to minimize the effects of beam damage. Due to multiple samples being analyzed during a typical run, the time between data collections for each sample was approximately 3 minutes.^[12] As presented in Figure 2, a rising temperature ramp of 1°Cmin⁻¹, starting from an initial temperature of 35 °C, revealed the existence of four distinct thermotropic phases of 1a that are connected through three well-defined order-order transitions. More specifically, at the lowest temperature, a pure L phase is initially observed up to a temperature of 83°C, whereupon a new phase begins to grow in and becomes the only phase that is present at 117°C (see lowest panel of Figure 2a). By indexing the Bragg scattering peaks of the latter SAXS data, which are positioned at $q/q^* = \sqrt{5}$, $\sqrt{6}$, $\sqrt{7}$, $\sqrt{15}$, $\sqrt{19}$, $\sqrt{21}$, $\sqrt{24}$, and $\sqrt{54}$ ($q^* = 0.1045 \text{ Å}^{-1}$) (see Figure 2b), the identity of this new phase was established as being the hexagonal perforated lamellar (HPL) phase of $R\bar{3}m$ symmetry in which the minor domains that punctuate major domain lamellae are positioned relative to each other in an ABCA stacked arrangement.[14] This structural assignment also provided the HPL unit cell parameters of a = 7.5 nm and c = 16.4 nm for

8711



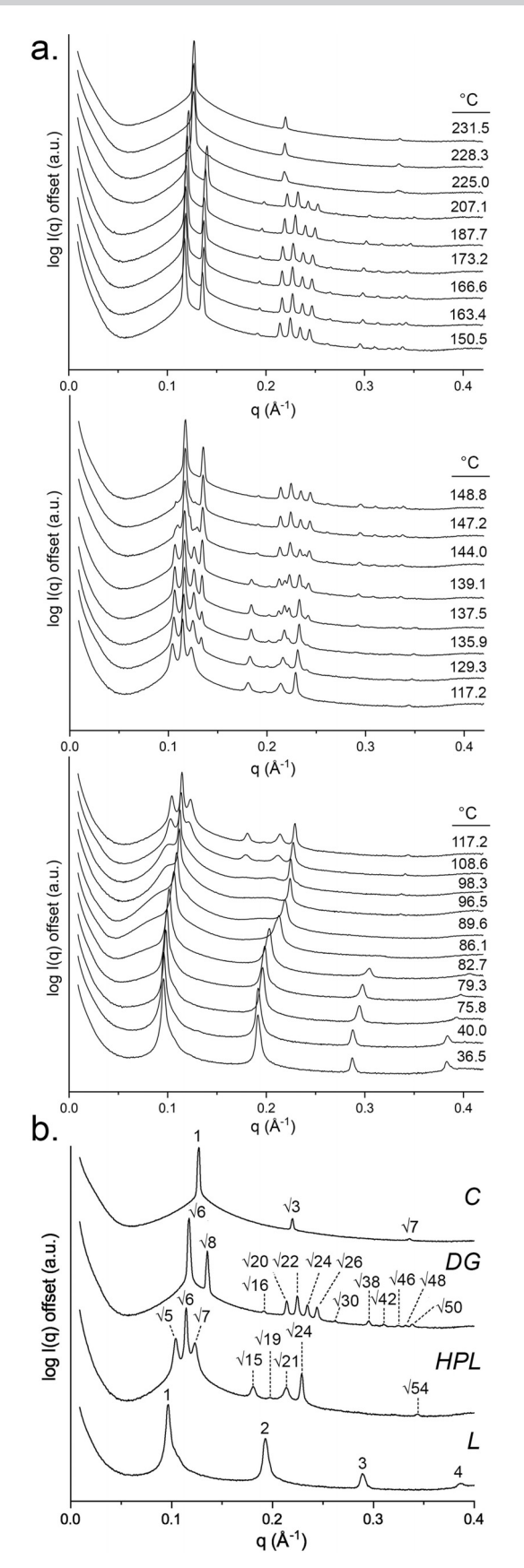


Figure 2. a) Selected VT SAXS data for a sample of 1 a. b) Structural assignments for pure phases obtained at temperatures shown in (a).^[12]

a c/a ratio of 2.19, which is very similar to c/a values reported for other ABCA-stacked HPL phases of microphase-separated block copolymers.[14,15]

Further heating of the HPL phase of 1a above 117°C resulted in the appearance of yet another phase, which becomes the only morphology that is present at 149°C (see middle panel of Figure 2a). Figure 2b also provides the results of a successful assignment of the new collection of fourteen scattering peaks that appear at $q/q^* = \sqrt{6}$, $\sqrt{8}$, $\sqrt{16}$, $\sqrt{20}$, $\sqrt{22}$, $\sqrt{24}$, $\sqrt{26}$, $\sqrt{30}$, $\sqrt{38}$, $\sqrt{42}$, $\sqrt{46}$, $\sqrt{48}$, and $\sqrt{50}$ $(q^* = 0.1175 \,\text{Å}^{-1})$ to a DG $(Ia\bar{3}d)$ phase with a unit cell length, a_{DG} , of 13.1 nm.^[5,7,15] Finally, as Figure 2 shows, the DG phase of 1a was found to be robust at higher temperatures, but above 207°C, it too undergoes an order-order transition into a hexagonal cylindrical (C) phase. For this final C morphology of 1a, the cylinder-to-cylinder distance, d_C , was calculated from the SAXS data of Figure 2b to be 5.75 nm at 225 °C ($q^* = 0.1263 \text{ Å}^{-1}$). [12] Additional structural information for the DG phase of 1a was obtained through a le Bail refinement of the SAXS data using the JANA 2006 program to provide a calculated set of hkl reflections and intensities that were then used as input for a SUPERFLIP computational reconstruction of three-dimensional electron density.^[16] Figure 3 displays the result for one such reconstruction of the DG phase in which the strut width for the interpenetrating sugar domain networks, as measured at the midpoint between two connected triangular intersections, is only 1.8 nm.

For block copolymers, theoretical studies have concluded that the HPL morphology is a metastable state, and experimentally, it has been observed as a long-lived intermediate involved in order-order transitions between two equilibrium mesophases. [14,15,17] On the other hand, the DGphase is now widely accepted as being a thermodynamic equilibrium morphology, but with only a small window of stability within the phase diagram of microphase-segregated block copolymers of varying segregation strength.^[5,17]

In the present work, it is reasonable to assume that the same epitaxial relationships that have been previously proposed and documented for thermotropic $L \leftrightarrow HPL$, $HPL \leftrightarrow DG$, and $DG \leftrightarrow C$ transitions in block copolymers

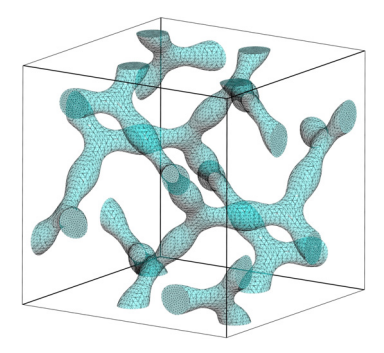


Figure 3. Reconstructed electron density map from SAXS data for the DG phase of $\bf 1\,a$ with a unit cell length, $a_{\rm DG}$, of 13.1 nm. The high electron density region (aqua) is associated with the sugar domain that forms two enantiomorphic interpenetrating networks with a strut width at the midpoint between two triangular intersections of 1.8 nm, while the white region of low electron density encompasses the polyolefin domain.

and other soft materials are also operative in the phase behavior displayed in Figure 2.[15] However, a unique feature of the order-order transitions involving 1a is that all three appear to be irreversible, or at a minimum, the reverse $C \rightarrow$ DG, $DG \rightarrow HPL$ and $HPL \rightarrow L$ processes are extremely slow. Accordingly, it was determined that pure bulk samples of the HPL and DG mesophase of 1a can be selectively prepared by simply annealing the material in vacuo at the proper temperature for a fixed period of time, and once formed, both phases were shown to be stable at ambient temperature for at least three months.^[12] On the other hand, a very preliminary study of the dependence of the stability of the DG phase as a function of humidity revealed that it rapidly reverts back to the L phase when exposed to $\geq 40\%$ relative humidity. This result suggests that dehydration of the cellobiose polar domains might serve to "lock-in" the different phases of 1a that are observed at increasing temperature. A more thorough investigation of the stability of all the thermotropic phases of **1a** over much longer periods of time and under a variety of environmental conditions is currently in progress.

Robust, highly ordered ultrathin films of DG phases are of particular interest for potential nanotechnological applications that include, for instance, nanoporous membranes and gating layers that can mediate selective high density proton, electron, and ion conduction. [6d,18] Unfortunately, due to strong surface energy and interface effects that can conspire to override thermodynamic stability, a soft matter DG phase has not been previously observed within sub-100-nm thick films in the absence of pre- or post-modification of surface energies of the supporting substrates and the air-film interface using bottom and top coats of a different material, or under tightly controlled environmental conditions. [7f,19]

Further, while bulk thermotropic DG phases have been previously observed for glycolipids, [5,13d] to the best of our knowledge, this same nanostructured morphology has not yet been reported for any class of saccharide-hydrocarbon within an ultra-thin film construct. Accordingly, a variable temperature synchrotron 2D GISAXS investigation of ultrathin films of $\mathbf{1a}$ that are supported on hydrophobic c-Si substrates was conducted using various temperature ramp and jump profiles in order to determine if the unique stability observed in the bulk for the HPL and DG phases also occurs in ultrathin films.

Figure 4 summarizes the results of a variable temperature GISAXS investigation of a freshly prepared 65-nm-thick film of **1a** spun cast onto a c-Si substrate using a 1% (wt/wt) solution of the sugar-polyolefin conjugate in a 1:1 n-butanol/hexanes solvent mixture (v/v) and a photoresist spin caster set at 2000 rpm under ambient conditions. Similar studies were also performed for 15-nm and 150-nm thick films for which solvent concentration was varied to establish different film thicknesses. [12] To begin, as schematically presented in Figure 4a, a temperature ramp performed between 35 °C to 250 °C at a rate of 1 °Cmin⁻¹ revealed the same sequence of four thermotropic phases of **1a** through well-defined orderorder transitions occurring approximately within the same temperature ranges as observed in bulk samples. The Supporting Information provides further details of represen-

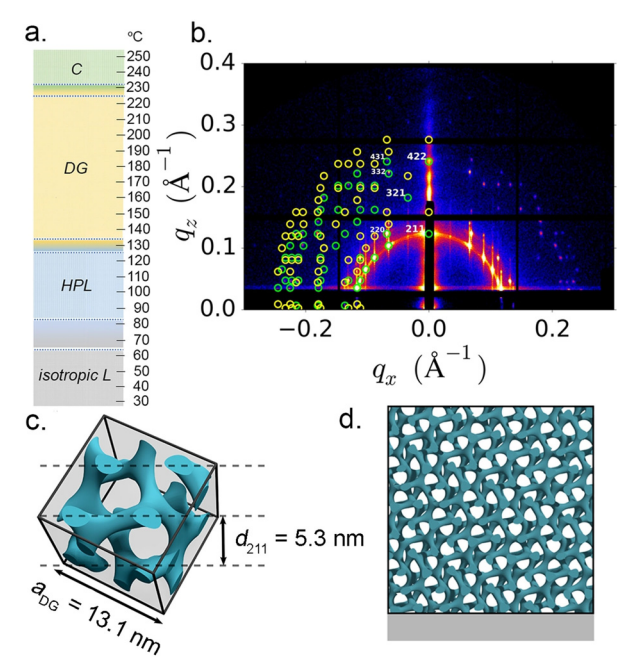
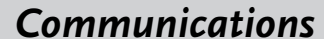


Figure 4. Synchrotron 2D GISAXS data for a 65-nm-thick ultrathin film of the DG phase of 1a supported on a carbon-coated silicon substrate. a) Observed phases as a function of temperature obtained starting at 35 °C and a temperature ramp of 1 °C min $^{-1}$. b) Indexed 2D GISAXS data for DG phase recorded at 150 °C with green and yellow circles indicating predicted locations of scattering Bragg peaks originating from the direct and reflected x-ray beam, respectively. c) Unit cell and lattice parameters for the DG phase derived from the GISAXS data of (b). d) Structural representation of an ultrathin film of the DG phase of 1a with the (211) Miller plane oriented parallel to the surface of the substrate.

tative GISAXS data obtained for each phase and the kinetics for each order-to-order phase transition of 1a (see Figures S18-S20). An added structural feature obtained from the successful indexing of these GISAXS data is orientation of the respective unit cell and extended lattice of the nanostructure relative to the substrate. More specifically, for all three film-thicknesses, an isotropically oriented L phase was first observed to emerge, followed by the HPL phase in which the alternating ABCA layers are oriented parallel to the substrate surface. With respect to the DG phase, the GISAXS data and structure results shown in Figure 4b and c for the 65nm-thick sample reveal a unit cell length that is identical to that of the bulk, and a lattice orientation in which the (211) Miller planes are parallel to the substrate. [12] Finally, the Cphase that appears upon heating the DG films to higher temperature consists of cylindrical domains that are also aligned parallel to the surface.

Some additional studies were conducted and important points can be made regarding the structures and stabilities of the different thermotropic phases observed for ultrathin films of 1a.^[12] To begin, pure sub-100-nm- thick HPL and DG phases that are highly ordered, surface-oriented, and exhibiting large grain size can be separately obtained by simply annealing the substrates in vacuo at the appropriate temperature for an adequate period. In this respect, the relative rates observed for the different order-order phase transitions are all







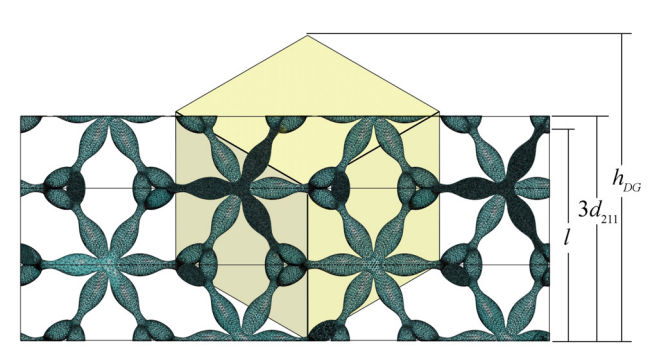


Figure 5. Representation of an ultrathin film of the DG phase of 1a with l=15 nm, $3\times d_{211}=15.9$ nm, and $h_{DG}=21.8$ nm as viewed along the (111) direction and with the (211) planes oriented parallel to the surface of the substrate. The sugar domain is shown in aqua while the white regions correlate with the polyolefin domain. A unit cell of the DG phase with the proper spatial orientation relative to the substrate, and translated arbitrarily along the surface normal for the sake of clarity, is shown in light yellow.

qualitatively slower than the corresponding transformations associated with a bulk sample. It further appears that these rates decrease with decreasing film thickness, suggesting that a nucleation and growth mechanism is operative. Most surprisingly, however, the unique long-term stability displayed by the DG phase of **1a** under ambient temperature can be extended to ultrathin films as thin as 15 nm! As Figure 5 presents, this value of l is now less than three times d_{211} , and accordingly, it is formally incommensurate with both an integer value of stacked (211) planes, as well as, the height, h_{DG} , that is required to accommodate one full unit cell of the DG nanostructure that is oriented relative to the substrate as shown. On the one hand, it is possible that this incommensurable difference between the value of l and the DG lattice and unit cell parameters is accommodated through an integerquantized inhomogeneity of film thickness of sample material across the substrate. [9] On the other hand, unequivocal documentation of an incommensurate nanostructure raises a number of interesting scientific questions and technological applications regarding a new category of two-dimensional Schoen TPMS nanostructures.

As a final consideration, we explored the question of how unique the results obtained for 1 might be with respect to: (1) the nature of the disaccharide head group, (2) the molar mass of the aPP tail, (3) potential secondary hydrogen-bonding interactions involving the triazole linker, and (4) the surface energy of the c-Si substrate used to support ultrathin films. Accordingly, Figure 6 provides a summary of VT GISAXS results obtained from an additional extensive series of experiments with the disaccharide-aPP derivatives 1-5 of Scheme 1 that serve to shed important additional light on the importance of these parameters.^[12] The Supporting Information has representative GISAXS data for each of the phases shown as a function of temperature, film thickness and substrate. To begin, three new derivatives of 1 were prepared in which the number-average degree of polymerization and polydispersity, DP_n of the aPP domain were determined to be 13 (**1b**), 31 (**1c**), and 62 (**1d**) as approximates for target molar mass of 500 Da, 1000 Da and 2500 Da, respectively. Film-

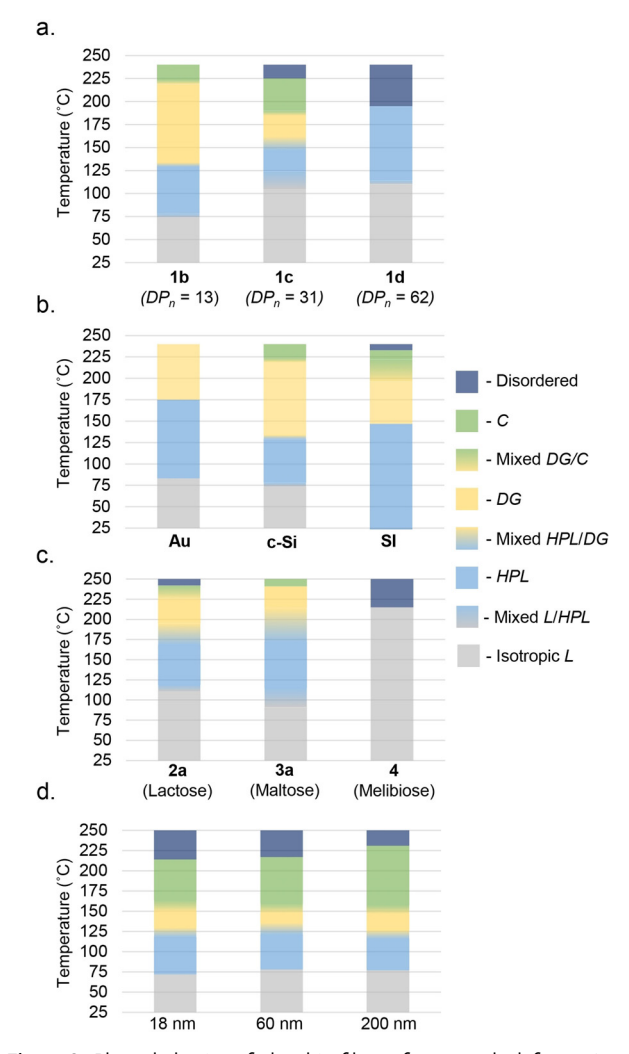


Figure 6. Phase behavior of ultrathin films of sugar-polyolefin conjugates as revealed by synchrotron VT GISAXS for a) 1 as a function of aPP chain length, b) 1a as a function of substrate, c) as a function of disaccharide head group and aPP chain length for 2–4 and d) as a function of linker for 5.

thickness dependences of the phase behaviour of 1b-1d were then determined by synchrotron VT GISAXS for film thicknesses of l=15 nm, 65 nm and 150 nm. Figure 6 a provides the results for the samples with l = 65 nm while the complete set of data is provided in the SI. Significantly, as can be seen, these studies revealed that the window for appearance of the DG phase decreases as the chain length and occupied volume of the aPP domain increases in going from 1b to 1c to 1d. On the other hand, it is very interesting to note that the window for appearance of a stable HPL phase also increases in the same order, such that ultrathin films of this unique phase can now be easily obtained with 1d at all values of l. Next, the phase behaviour of ultrathin films of $\mathbf{1a}$ for l =65 nm was determined for two additional surfaces, which include the hydrophilic native SiO2 layer of Si and the "neutral" surface of Au. Figure 6b presents a summary of the VT GISAXS data for this study which shows that all three surfaces were competent for supporting formation of stable HPL and DG nanostructures, with the windows for appear-





ance of these phases being only slightly dependent on the nature of substrate surface energy. Furthermore, in a different set of experiments, the disaccharide head group in the sugarpolyolefin conjugate was varied to include lactose (2), maltose (3) and melibiose (4) and for two different DP_n values of the aPP domain for the first two, which are 15 (series a) and 37 (series b). As Figure 6c establishes for 2a, 3a and 4, only the melibiose derivative, which has an α -1,6 linkage between the galactose and glucose units that enforces a very unique disaccharide conformation vis-à-vis those of the cellobiose, lactose and maltose head groups of 1-3, respectively, failed to provide either HPL or DG phases, and only a lamellar phase was observed at the three different film thicknesses investigated. [12] This result strongly suggests that differences in disaccharide head group packing and secondary hydrogen-bond interactions do play critical roles in dictating phase morphology. Additional VT SAXS data for 2b and 3b show that neither of these derivatives support the occurrence of a DG, and accordingly, a fine balance between the structure of the disaccharide head group and chain length of the aPP domain must be established when considering the design of other sugar-polyolefin conjugates. Finally, Figure 6d presents another rather surprising result from SAXS and VT GISAXS data which shows that the thermotropic phase behaviour of the ether-linked disaccharide derivative 5 (see Scheme 1) with $DP_n = 15$ is very similar to that of **1a**, including observation of a stable DG phase once again at the two-dimensional limit where l = 15 nm. Efforts are now in progress that can potentially shed further light on the structure and stability of Schoen DG nanostructures at this two-dimensional limit, as well as an exploration of potential applications.

Acknowledgements

This research used resources of the Center for Functional Nanomaterials and the National Synchrotron Light Source II, which are U.S. DOE Office of Science Facilities, at Brookhaven National Laboratory under Contract No. DE-SC0012704. We thank the National Science Foundation for support for the acquisition of SAXS and AFM instruments (DMR-1228957 and MRI 1626288, respectively) and high field 800 MHz and solid state 500 MHz NMR spectrometers (BDI-1040158 and MRI 1726058, respectively). Partial support of this work was also provided by the NSF (CHE-1955730) for which we are grateful.

Conflict of interest

The corresponding author has a financial stake in the university spin-out company, Precision Polyolefins, LLC (PPL). No PPL personnel, funding or resources were used in the research and all new IP has been disclosed according to federal and state requirements.

Keywords: gyroid · self-assembly · ultrathin film

- See, for instance: a) S. G. Lemay, Angew. Chem. Int. Ed. 2010, 49, 7627-7628; b) M. D. Ellison, S. Menges, L. Nebel, G. D'Arcangelo, A. Kramer, L. Drahushuk, J. Benck, S. Shimizu, M. S. Strano, J. Phys. Chem. C 2017, 121, 2005-2013; c) E. Hancox, E. Liarou, J. S. Town, G. R. Jones, S. A. Layton, S. Huband, M. J. Greenall, P. D. Topham, D. M. Haddleton, Polym. Chem. 2019, 10, 6254-6259; d) A. Xiao, Z. Zhang, X. Shi, Y. Wang, ACS Appl. Mater. Interfaces 2019, 11, 44783-44791; e) L. Barreda, Z. Shen, Q. P. Chen, T. P. Lodge, J. I. Siepmann, M. A. Hillmyer, Nano Lett. 2019, 19, 4458-4462.
- [2] a) C. Peroz, S. Dhuey, M. Cornet, M. Vogler, D. Olynick, S. Cabrini, *Nanotechnology* 2012, 23, 015305; b) G. S. Doerk, H. Gao, L. Wan, J. Lille, K. C. Patel, Y.-A. Chapuis, R. Ruiz, T. R. Albrecht, *Nanotechnology* 2015, 26, 085304; c) S. Ji, L. Wan, C.-C. Liu, P. F. Nealey, *Prog. Polym. Sci.* 2016, 54–55, 76–127.
- [3] A. H. Schoen, NASA Technical Note D-5541, 1970.
- [4] L. Han, S. Che, Adv. Mater. 2018, 30, 1705708.
- [5] For some leading references, see: a) V. Luzzati, P. A. Spegt, Nature 1967, 215, 701-704; b) D. A. Hajduk, P. E. Harper, S. M. Gruner, C. C. Honeker, G. Kim, E. L. Thomas, L. J. Fetters, Macromolecules 1994, 27, 4063-4075; c) D. A. Davidock, M. A. Hillmyer, T. P. Lodge, Macromolecules 2003, 36, 4682-4685; d) R. Hashim, A. Sugimura, H. Minamikawa, T. Heidelberg, Liq. Cryst. 2012, 39, 1-17; e) X. Yu, K. Yue, I.-F. Hsieh, Y. Li, X.-H. Dong, C. Liu, Y. Xin, H.-F. Wang, A.-C. Shi, G. R. Newkome, R.-M. Ho, E.-Q. Chen, W.-B. Zhang, S. Z. D. Cheng, Proc. Natl. Acad. Sci. USA 2013, 110, 10078-10083; f) C. Tschierske, Angew. Chem. Int. Ed. 2013, 52, 8828-8878; g) X. Feng, C. J. Burke, M. Zhuo, H. Guo, K. Yang, A. Reddy, I. Prasad, R.-M. Ho, A. Avgeropoulos, G. M. Grason, E. L. Thomas, Nature 2019, 575, 175-179.
- [6] See, for instance: a) V. N. Urade, T.-C. Wei, M. P. Tate, J. D. Kowalski, H. W. Hillhouse, *Chem. Mater.* 2007, 19, 768-777;
 b) D. Wei, M. R. J. Scherer, C. Bower, P. Andrew, T. Ryhänen, U. Steiner, *Nano Lett.* 2012, 12, 1857-1862; c) J. A. Dolan, B. D. Wilts, S. Vignolini, J. J. Baumberg, U. Steiner, T. D. Wilkinson, *Adv. Opt. Mater.* 2015, 3, 12-32; d) H.-Y. Hsueh, C.-T. Yao, R.-M. Ho, *Chem. Soc. Rev.* 2015, 44, 1974-2018; e) L. Wu, W. Zhang, D. Zhang, *Small* 2015, 11, 5004-5022; f) M. R. J. Scherer, U. Steiner, *Nano Lett.* 2013, 13, 3005-3010; g) J. G. Werner, G. G. Rodríguez-Calero, H. D. Abruña, U. Wiesner, *Energy Environ. Sci.* 2018, 11, 1261-1270.
- [7] a) J. Jung, H.-W. Park, S. Lee, H. Lee, T. Chang, K. Matsunaga, H. Jinnai, ACS Nano 2010, 4, 3109-3116; b) M. Luo, J. E. Seppala, J. N. Albert, R. L. Lewis III, N. Mahadevapuram, G. E. Stein, T. H. Epps III, Macromolecules 2013, 46, 1803-1811; c) S. Park, Y. Kim, W. Lee, S.-M. Hur, D. Y. Ryu, Macromolecules 2017, 50, 5033-5041; d) K. Aissou, M. Mumtaz, G. Portale, C. Brochon, E. Cloutet, G. Fleury, G. Hadziioannou, Small 2017, 13, 1603777; e) C.-H. Hsu, K. Yue, J. Wang, X.-H. Dong, Y. Xia, Z. Jiang, E. L. Thomas, S. Z. D. Cheng, Macromolecules 2017, 50, 7282-7290; f) I. Ryu, Y. J. Kim, Y. S. Jung, J. S. Lim, C. A. Ross, J. G. Son, ACS Appl. Mater. Interfaces 2017, 9, 17427-17434; g) T. Wen, H.-F. Wang, P. Georgopanos, A. Avgeropoulos, R.-M. Ho, Polymer 2019, 167, 209-214.
- [8] a) D. F. Sunday, M. J. Maher, S. Tein, M. C. Carlson, C. J. Ellison, C. G. Willson, R. J. Kline, ACS Macro Lett. 2016, 5, 1306-1311;
 b) S. Kim, W. Li, G. H. Fredrickson, C. J. Hawker, E. J. Kramer, Soft Matter 2016, 12, 5912-5925;
 c) H. S. Suh, D. H. Kim, P. Moni, S. Xiong, L. E. Ocola, J. J. Zaluzec, K. K. Gleason, P. F. Nealey, Nat. Nanotechnol. 2017, 12, 575-581.
- [9] T. P. Russell, Y. Chai, Macromolecules 2017, 50, 4597 4609.
- [10] a) T. S. Thomas, W. Hwang, L. R. Sita, Angew. Chem. Int. Ed.
 2016, 55, 4683-4687; b) S. R. Nowak, W. Hwang, L. R. Sita, J.
 Am. Chem. Soc. 2017, 139, 5281-5284; c) K. K. Lachmayr, C. M.
 Wentz, L. R. Sita, Angew. Chem. Int. Ed. 2020, 59, 1521-1526;

8715





- d) K. K. Lachmayr, L. R. Sita, *Angew. Chem. Int. Ed.* **2020**, *59*, 3563 3567.
- [11] a) W. Zhang, L. R. Sita, J. Am. Chem. Soc. 2008, 130, 442-443;
 b) W. Zhang, J. Wei, L. R. Sita, Macromolecules 2008, 41, 7829-7833
- [12] Details are provided in the Supporting Information.
- [13] Highly ordered nanostructured films with sub-10-nm feature size have been reported for other saccharide-polymer materials, see for instance: a) J. D. Cushen, I. Otsuka, C. M. Bates, S. Halila, S. Fort, C. Rochas, J. A. Easley, E. L. Rausch, A. Thio, R. Borsali, C. G. Willson, E. J. Ellison, ACS Nano 2012, 6, 3424–3433; b) I. Otsuka, N. Nilsson, D. B. Suyatin, I. Maximov, R. Borsali, Soft Matter 2017, 13, 7406–7411; c) T. Isono, B. J. Ree, K. Tajima, R. Borsali, T. Satoh, Macromolecules 2018, 51, 428–437; d) K. Yoshida, S. Tanaka, T. Yamamoto, K. Tajima, R. Borsali, T. Isono, T. Satoh, Macromolecules 2018, 51, 8870–8877; e) T.-H. Chuang, Y.-C. Chiang, H.-C. Hsieh, T. Isono, C.-W. Huang, R. Borsali, T. Satoh, W.-C. Chen, ACS Appl. Mater. Interfaces 2020, 12, 23217–23224; f) T. Isono, R. Komaki, C. Lee, N. Kawakami, B. J. Ree, K. Watanabe, K. Yoshida, H. Mamiya, T. Yamamoto, R. Borsali, K. Tajima, T. Satoh, Commun. Chem. 2020, 3, 135.
- [14] For previous reports of the HPL phase morpology, see: a) I. W. Hamley, K. A. Koppi, J. H. Rosedale, F. S. Bates, K. Almdal, K. Mortensen, Macromolecules 1993, 26, 5959-5970; b) S. Förster, A. K. Khandpur, J. Zhao, F. S. Bates, I. W. Hamley, A. J. Ryan, W. Bras, Macromolecules 1994, 27, 6922-6935; c) D. A. Hajduk, H. Takenouchi, M. A. Hillmyer, F. S. Bates, M. E. Vigild, K. Almdal, Macromolecules 1997, 30, 3788-3795; d) L. Zhu, P. Huang, S. Z. D. Cheng, Q. Ge, R. P. Quirk, E. L. Thomas, B. Lotz, J.-C. Wittman, B. S. Hsiao, F. Yeh, L. Liu, Phys. Rev. Lett. 2001, 86, 6030-6033; e) J.-H. Ahn, W.-C. Zin, Macromolecules 2000, 33, 641-644; f) Y. L. Loo, R. A. Register, D. H. Adamson, A. J. Ryan, Macromolecules 2005, 38, 4947-4949; g) N. Zhou, T. P. Lodge, F. S. Bates, Soft Matter 2010, 6, 1281-1290.
- [15] a) M. F. Schulz, F. S. Bates, K. Almdal, K. Mortensen, *Phys. Rev. Lett.* **1994**, *73*, 86–89; b) D. A. Hajduk, R.-M. Ho, M. A.

- Hillmyer, F. S. Bates, K. Almdal, *J. Phys. Chem. B* **1998**, *102*, 1356–1363; c) M. E. Vigild, K. Almdal, K. Mortensen, I. W. Hamley, J. P. A. Fairclough, A. J. Ryan, *Macromolecules* **1998**, *31*, 5702–5716; d) M. Imai, K. Sakai, M. Kikuchi, K. Nakaya, A. Saeki, T. Teramoto, *J. Chem. Phys.* **2005**, *122*, 214906; e) C. Lai, Y.-L. Loo, R. A. Register, D. H. Adamson, *Macromolecules* **2005**, *38*, 7098–7104; f) I. Park, B. Lee, J. Ryu, K. Im, J. Yoon, M. Ree, T. Chang, *Macromolecules* **2005**, *38*, 10532–10536; g) H.-W. Park, K. Im, B. Chung, M. Ree, T. Chang, K. Sawa, H. Jinnai, *Macromolecules* **2007**, *40*, 2603–2605; h) V. H. Mareau, S. Akasaka, T. Osaka, H. Hasegawa, *Macromolecules* **2007**, *40*, 9032–9039.
- [16] a) V. Petricek, M. Dusek, L. Palatinus, Z. Kristallogr. 2014, 229, 345–352; b) L. Palatinus, G. Chapius, J. Appl. Crystallogr. 2007, 40, 786–790.
- [17] a) M. W. Matsen, F. S. Bates, Macromolecules 1996, 29, 1091–1098; b) K. Yamada, M. Nomura, A. Saeki, T. Ohta, J. Phys. Chem. Condens. Matter 2005, 17, 4877–4887; c) E. W. Cochran, C. J. Garcia-Cervera, G. H. Fredrickson, Macromolecules 2006, 39, 2449–2451; d) N. Ji, P. Tang, F. Qiu, A.-C. Shi, Macromolecules 2015, 48, 8681–8693.
- [18] See for instance: a) L. Li, P. Szewczykowski, L. D. Clausen, K. M. Hansen, G. E. Jonsson, S. Ndoni, J. Membrane Sci. 2011, 384, 126–135; b) L. Li, L. Schulte, L. D. Clausen, K. M. Hansen, G. E. Jonsson, S. Ndoni, ACS Nano 2011, 5, 7754–7766; c) L. Yan, C. Rank, S. Mecking, K. I. Winey, J. Am. Chem. Soc. 2020, 142, 857–866.
- [19] M. Rittman, H. Amenitsch, M. Rappolt, B. Sartori, B. M. D. O'Driscoll, A. M. Squires, *Langmuir* 2013, 29, 9874–9880.

Manuscript received: December 9, 2020 Accepted manuscript online: February 10, 2021 Version of record online: March 8, 2021